Journal of Geology and Mining Research Vol. 1(1) pp. 008-018 March, 2009
Available online http://www.academicjournals.org/jgmr
©2009 Academic Journals

Full Length Research Paper

Geoelectric mapping and characterization of limestone deposits of Ewekoro formation, southwestern Nigeria

B. S. Badmus[1]* and O. B. Olatinsu[2]

[1]Department of Physics, University of Agriculture, Abeokuta, Nigeria.
[2]Department of Physics, University of Lagos, Lagos, Nigeria.

Accepted 17 February, 2009

62 vertical electrical soundings (VES) were carried out to map limestone deposits of Ewekoro formation, south-western Nigeria. The maximum current electrode spacing AB/2 was 1 km. The results revealed the occurrence of limestone in all the locations within the third and fourth geoelectric layers with resistivity values ranging from 10 to 100 KΩm and thickness range of 15 to 90 m. The resistivity values of the limestone samples collected from the study site were also analyzed by laboratory direct method. This direct method revealed that the resistivity values fall within 6 and 171 KΩm. The two approaches showed a good degree of correlation in the resistivity value of the limestone and their varying qualities. This research work further showed the occurrence of vast deposit of limestone, which can be of economic importance in mining and industrial purposes.

Key words: Resistivity, limestone, geoelectric layer, permeability, Ewekoro formation.

INTRODUCTION

Geophysical exploration was carried out to map the limestone deposit of Ewekoro formation using two different approaches: the vertical electrical sounding (VES) via Schlumberger arrangement and direct laboratory method via direct current power supply. The direct method approach is to complement and compare the study carried out by Badmus and Ayolabi (2005) where limestone of Ewekoro formation was delineated using Schlumberger electrode array to map both vertical and lateral extents of the deposit (Figure 1). This approach would also confirm the accuracy of electrical resistivity method of geophysical prospecting for mineral exploration as well as characterizing the various litho-facies of Ewekoro limestone (Badmus and Ayolabi, 2005). Balm's et al. (2006) carried out geoelectric evaluation of mica schist deposit of Area J4, southwestern, Nigeria using the direct laboratory method to characterize the mica schist into different degrees of purity for both economic and commercial purposes. This mineral exploration work was carried out to analyse both the electrical and physical parameters of limestone in Ewekoro formation. Several studies have also been carried out to evaluate the distribution of limestone deposits at Ewekoro quarry. Adegoke et al. (1970) subdivided the limestone deposits into three units. Omatosola and Adegoke (1981) then proposed a fourth unit. These units in stratigraphic order are: sandy biomcrosparite (bottom), shelly biomcrite, algal biosparite and red phosphate biomcrite (top). The sandy biomcrosparite forms the base of the formation and consists of a light brown sandy limestone with very few bioclassic fragments. Stratification is evident and is accentuated by variations in the quantity and grain size of the interbedded quartz and glauconite. The shelly biomcrite consists of pure limestone of about 4.5 to 6.0 m and constitute the bulk of the Ewekoro formation in the quarry. Limestone has abundant macrofossil content particularly gastropods, pelecypods, echinoderms and corals. The algal biosparite limestone overlies the shelly biomcrite unit. Resistivity is the only electrical characteristic of geoelectric property. Most rock forming minerals have conductivities spreading over a wide range and are semiconductors. However, these rocks are seen as insulators in their dried form. The amount of moisture contained in the rock depends on the structure especially the amount of pore space and cracks. Rocks and sediments contain space between grains (pore space) in fractures or in dissolved cavities (limestone), which may be filled with water. The porosity and chemical content of the water filling the pore

*Corresponding author. E-mail: badmusbs@yahoo.co.uk.

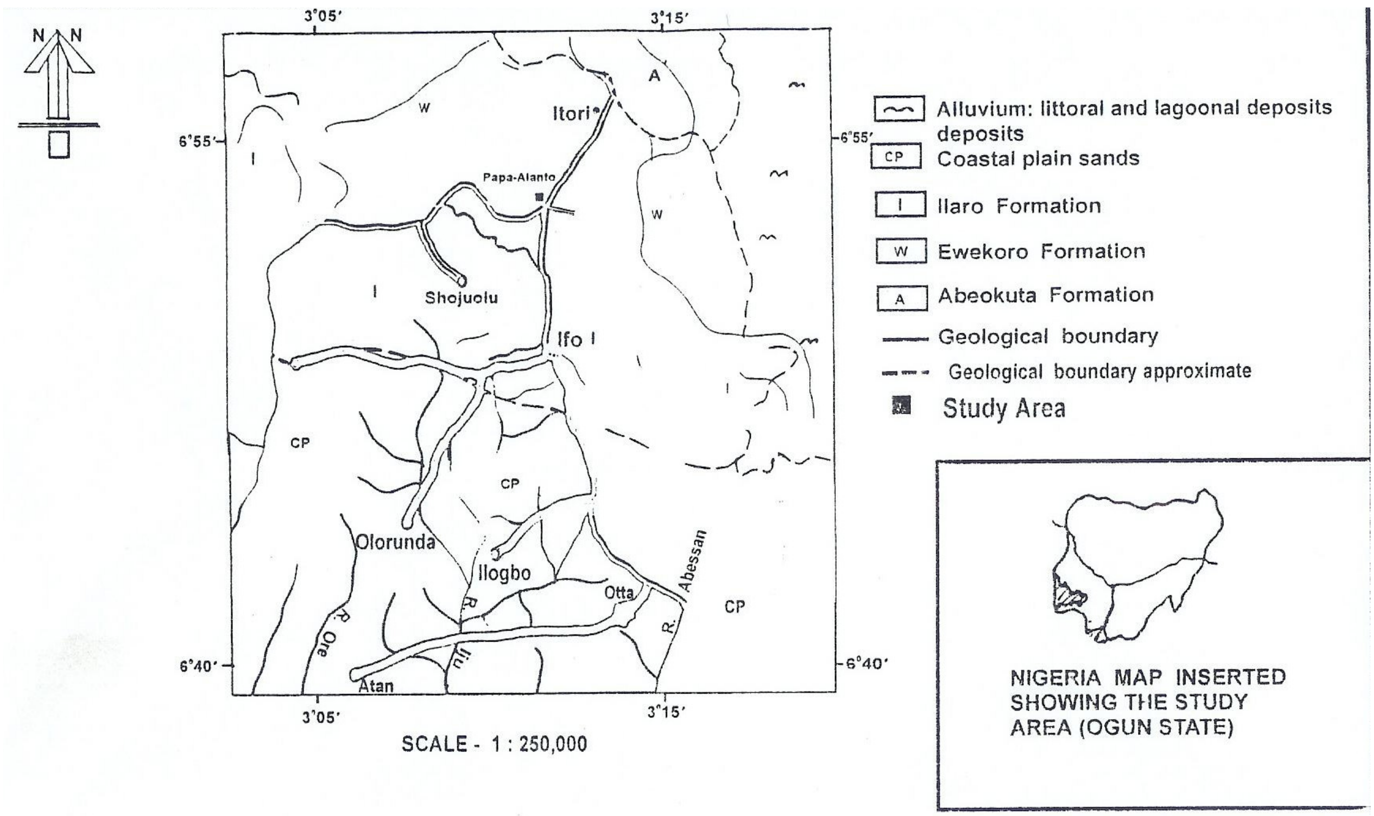

Figure 1. Geological map of Papa-Alanto and its environ (Bulletin: Geological Survery, Nigeria, No. 31, R. D. Hockey, H. A. Jones and J. D. Carter, 1957-61).

spaces are more important in governing resistivity than conductivity of the mineral grains of which the rock is composed.

Limestone is a raw material for the manufacturing of cement, asphalt filler, ceramics, flux in glass making, fertilizer filler, explosives to mention just a few. Jones and Hockey (1964) revealed Ewekoro limestone and the overlying Akinbo shale to be lateral equivalents of the Imo formation of eastern Nigeria. Other authors such as Omatsola and Adegoke (1991) and Oladeji (1992) have investigated the stratigraphy and depositional character-ristics of limestone and clay/shale deposits in south-western Nigeria. The West African Portland Cement Company also conducted extensive geological survey and commercial appraisal of Ewekoro limestone and shale beds for commercial cement production.

STUDY AREA

The study area lies within Ogun State, which is bounded in the west by Benin Republic, in the south by Lagos State, in the north by Oyo and Osun States, and in the east by Ondo State. It occupies a total area of 16,400 km^2. Ewekoro is the host to West African Portland Cement quarry and lies between longitude 3° 05´E to 3° 15´E and latitudes 6° 40´N to 6° 55´N (Figure 1).

GEOLOGY OF THE STUDY AREA

The study area is located in the sedimentary area of south-western Nigeria. Ewekoro formation belongs to tertiary formed Paleocene and Eocene; and the greater part of the depression is a potential artesian basin where ground water can be sourced. Kogbe (1976) and Adegoke et al. (1972) described the stratigrahpic and paleography of different sedimentary basins. Adegoke et al. (1976) outlined the Albran and younger Paleographic history of Nigeria and summarized the nature and extent of transgressive, regressive phases as well as the nature of the sediment.

The geology of Ogun State comprises sedimentary and basement complex rocks, which underlie the remaining surface area of the state. It also consists of intercalations of argillaceous sediment. The rock is soft and friable but in some places cement by ferruginous and siliceous materials. The sedimentary rock of Ogun State consists of Abeokuta formation lying directly above the basement complex (Figure 1). This in turn is overlain by Ewekoro, Oshosun and Ilaro formations, which are all overlain by the coastal plain sands (Benin formation).

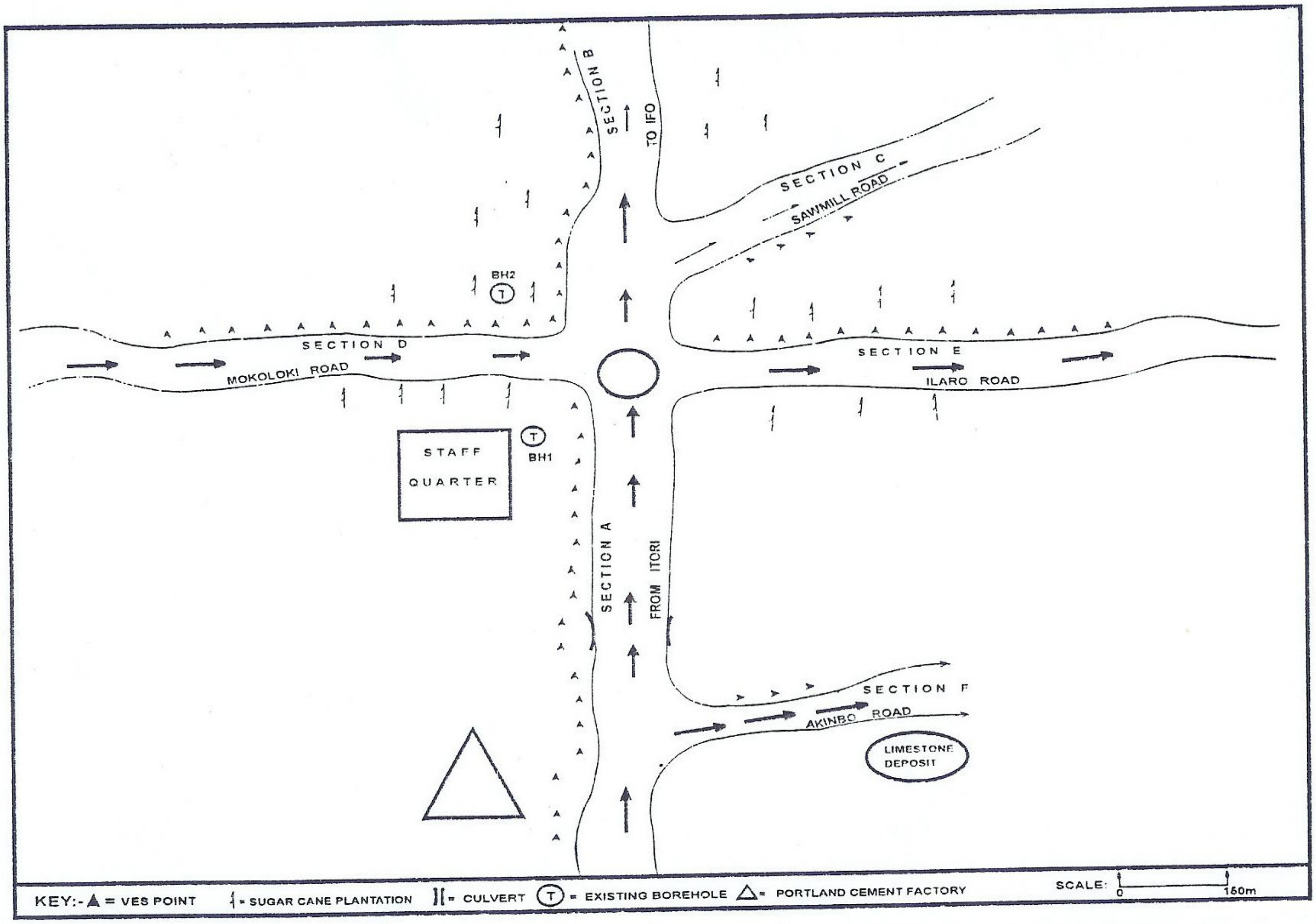

Figure 2. Data acquisition map.

METHODS

Electrical resistivity method

The vertical and lateral distribution of limestone in Ewekoro was investtigated using the electrical resistivity method. 62 vertical electrical soundings (VES) were carried out using the Schlumberger electrode configuration (Figure 4). Schlumberger array was used because of its greater depth penetration, (Ojelabi et al., 2002). The VES stations were arranged based on observable limestone outcrops found within the vicinity of the study area and were divided into six profiles (Figure 2). These profiles are: A (VES 01-17); B (VES 18-30); C (VES 31-34); D (VES 35-46); E (VES 47-59); and F (VES 60-62). The maximum current and potential electrodes spacing were 1 km and 30 m respectively, while the VES stations were separated by 150 m. The ABEM Terrameter 300B and its accessories were used for data acquisition. The apparent resistivity values obtained from the Terrameter were plotted against half the current electrode spacing (AB/2) on a log-log graph (Figure 3). Partial curve matching (a graphical procedure for semi-empirical interpretation of resistivity sounding data) was adopted to obtain model parameters for quantitative interpretation.

Direct laboratory measurement using d.c supply

Resistivity of limestone samples collected from the study area were analysed using a simple laboratory experimental set-up (Figure 5). The limestone samples collected were ground and packed into a core sampler of cylindrical shape and saturated hydraulically for 24 h. After which they were dried in the oven to remove completely the water content in the samples and were shaped into regular forms so as to make good contact with the pins (connecting wires) inserted into the samples. Direct current source was used to supply voltage across the two ends of the core sampler. Voltage was supplied at 12 and 24 V and the corresponding currents were recorded (Table 2).

RESULTS AND DISCUSSIONS

Geoelectric mapping

The results of the VES sounding at each of the profiles showed sounding curves with 4- to 7-layered types as revealed by the computer iteration techniques. The interpreted results revealed the presence of 4 geoelectric layers, while only a few revealed the presence of 5 or 6 geoelectric layers (Figure 3). The resistivity values from field procedure range between 10-100 kΩm as shown in the work of Badmus and Ayolabi (2005).

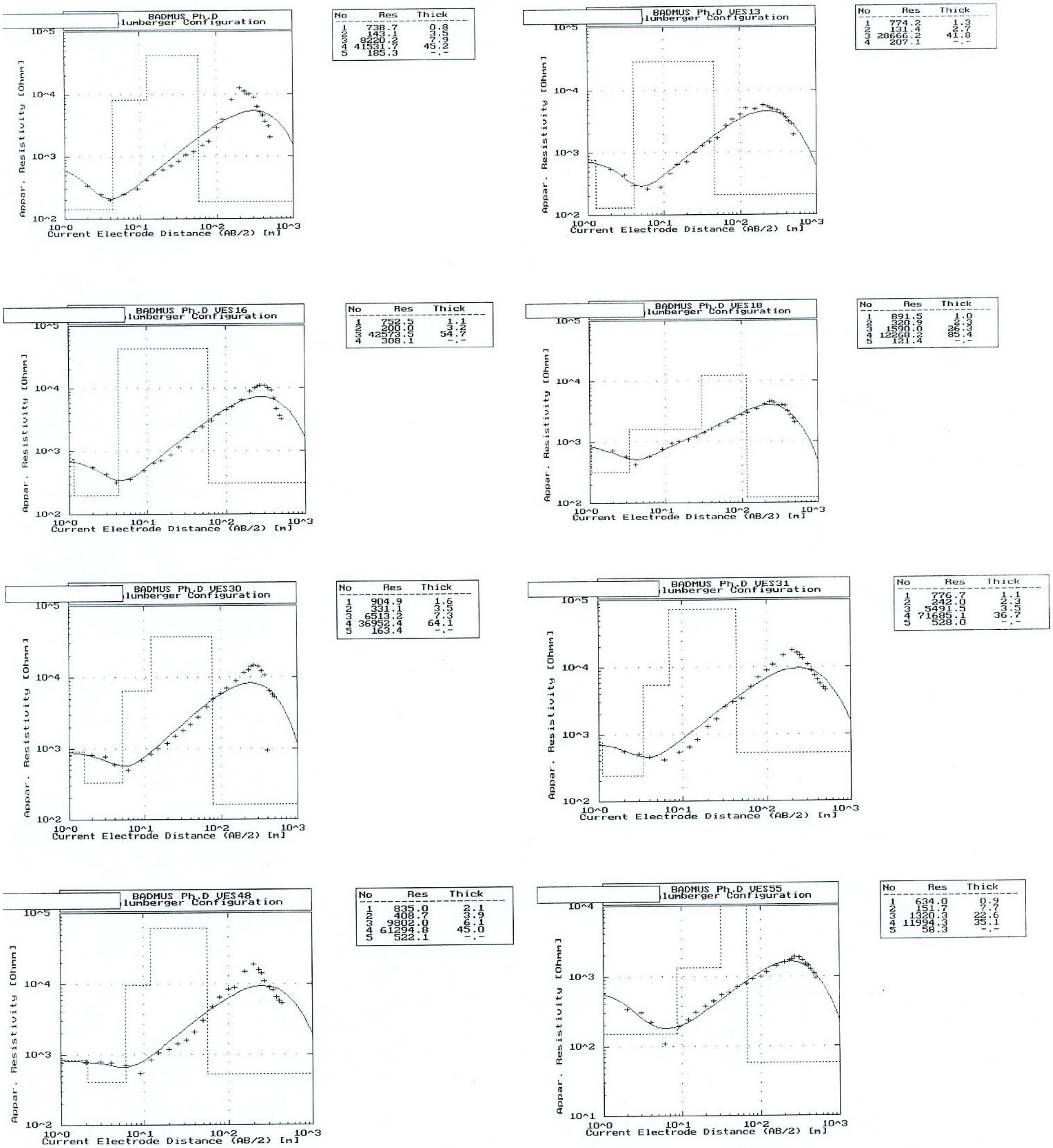

Figure 3. Computer modeling for some selected sounded stations.

Profile A (VES 01 – 17): This profile reveals the presence of limestone of 2 different litho-facies mainly in the third and fourth geoelectric layers. The resistivity ranges from 12 to 44 kΩm and thickness between 18.8 and 61.0 m as shown in Table 1.

Profile B (VES 18 – 30): Here, 2 different facies of limestone were delineated in the third and fourth geoelectric

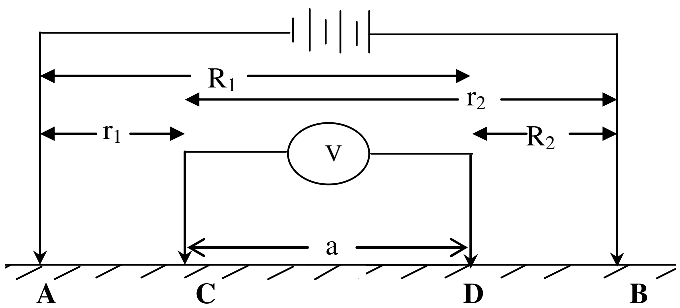

Figure 4. Schlumberger electrode arrangement

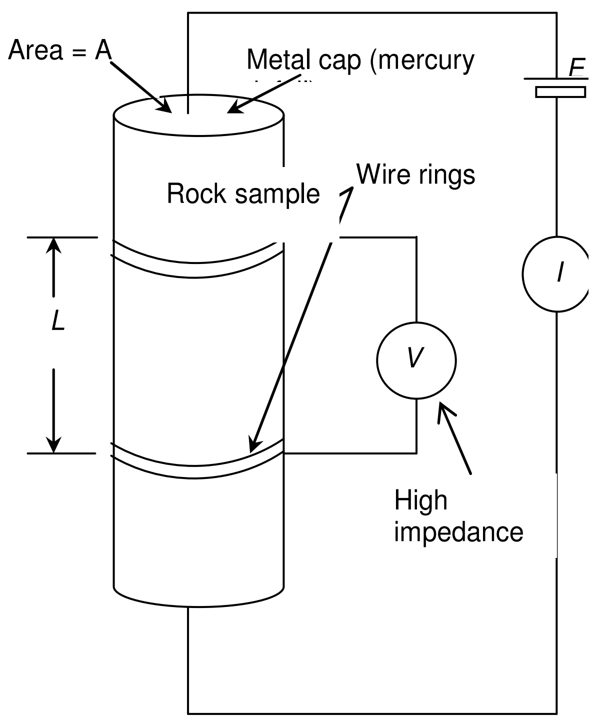

Figure 5. Direct method experimental setup.

layers with resistivity ranging from 12 to 63 kΩm and the thickness from 5 to 90 m (Table 1).

Profile C (VES 31 – 34): All the VES locations have 5 geoelectric layers except VES 34 which has only 4 geoelectric layers. Limestone was delineated in the fourth layer, with the resistivity ranging from 28 to 72 kΩm and the thickness between 37 and 66 m (Table 1).

Profile D (VES 35 – 46): Limestone occurrence was found in the third geoelectric layer except in 4 VES locations (35, 36, 42, and 43) where limestone was delineated in the fourth geoelectric layer. Here the limestone resistivity ranges from 19 to 100 kΩm and the thickness is quite appreciable from 23 to 72m. Two litho-facies also exist along this profile as shown in Table 1.

Profile E (VES 47 – 59): Along this profile, there are 4 geoelectric layers beneath 8 VES locations (47, 49, 50, 54, 56 - 59) and 5 geoelectric layers beneath the remaining 5 VES locations (48, 51, 52, 53, and 55). Limestone occurrence was found in 13 of the VES locations in the third and fourth geoelectric layers. The resistivity of these layers range from 10.3 to 96 kΩm and their thickness from 15 to 81 m (Table 1).

Profile F (VES 60 – 62): This profile has only 3 VES locations (60, 61, and 62). A minimum of 4 and a maximum of 5 geoelectric layers were delineated along the profile. Limestone occurred in the third and fourth geoelectric layers with resistivity values ranging from 11 to 95 kΩm and thickness between 15 and 61 m (Table 1).

Contour maps

Contour mapping is one of the techniques that can be used for interpretation of resistivity data. Limestone distribution of the study area was contoured using a computer software, “Suffer” and 3 types of contour maps were prepared for the study (Figures 6a - c). The limestone overburden thickness (Figure 6a) showed clearly the depth of the limestone in all the profile. Since overburden thickness composed of all materials above the limestone bed, it shows that limestone deposit appear at various depths along the study area. This contour shows a region of thick overburden/depression, indicated by dense contour closures along the central and eastern parts of the study area. However, regions of thin overburden/depression are found along the western and some in the eastern parts, where limestone could be easily explored.

The limestone thickness map (Figure 6b) showed various thicknesses of all locations sounded and also envisaged the reserve capacity of the limestone within the area. Region of possible fractures/deep-seated faults are depicted by widely spaced closed contour lines, showing the vertical lateral distribution of the limestone within the study area. The resistivity contour map (Figure 6c) however, showed the spatial distribution of resistivity across the study area.

Geoelectric profile

The geoelectric profiles of some typical sections along the study area are shown in Figure 7 (a – d). These revealed to a large extent a good quantity of limestone composition, which is of economic importance in mining and industrial purposes. However, in exploring for limestone, certain environmental and engineering safety precautions should be put in place as the resistivity results depict the existence of groundwater aquifers underlying the limestone beds. Because if all the limestone is totally excavated, the whole area would be flooded as the limestone bed serves as the overlaying rock for groundwater accumulation.

Table 1. Results obtained from field measurement.

Location	Longitude	Latitude	Overburden thickness (m)	Limestone Thickness (m)	Limestone Resistivity (kΩ-m)
VES 01	3.2070	6.9047	14.1	29.8	33.7
VES 02	3.1987	6.9049	9.8	61.0	36.7
VES 03	3.2096	6.9095	2.8	18.8	36.7
VES 04	3.1986	6.8924	-	-	-
VES 05	3.1984	6.8922	5.0	50.8	32.8
VES 06	3.2018	6.8971	6.1	39.2	31.6
VES 07	3.1985	6.9084	-	-	-
VES 08	3.2024	6.9090	7.8	47.8	44.0
VES 09	3.1927	6.8947	12.2	45.2	41.5
VES 10	3.1927	6.8958	6.9	38.2	18.0
VES 11	3.2019	6.9070	3.6	20.7	11.6
VES 12	3.1850	6.9032	2.3	36.1	17.6
VES 13	3.2098	6.8908	4.0	41.8	28.7
VES 14	3.1855	6.9053	69.8	47.3	12.1
VES 15	3.2007	6.8902	3.8	39.4	41.6
VES 16	3.1859	6.8987	4.3	54.7	42.6
VES 17	3.2012	6.8850	16.9	44.2	18.1
Value range (profile A)			2.3-69.8	18.8-61.0	11.6-44.0
VES 18	3.1925	6.8834	29.6	85.4	12.3
VES 19	3.1922	6.8828	2.3	5.1	12.6
VES 20	3.1930	6.8840	26.3	53.2	29.3
VES 21	3.1920	6.8819	14.6	46.9	36.2
VES 22	3.1924	6,8835	4.3	35.0	63.4
VES 23	3.1925	6.8819	12.0	41.3	20.5
VES 24	3.1931	6.8840	17.4	41.7	17.6
VES 25	3.1914	6.8821	6.5	60.9	17.7
VES 26	3.1924	6.8830	16.5	40.7	24.5
VES 27	3.1920	6.8819	12.5	64.3	40.9
VES 28	3.1929	6.8828	6.6	89.8	25.0
VES 29	3.1929	6.8840	13.3	43.8	35.9
VES 30	3.1922	6.8829	12.4	64.1	37.0
Values Range (Profile B)			2.3-29.6	5.1-89.8	12.3-63.4
VES 31	3.1924	6.8838	6.9	36.7	71.7
VES 32	3.1923	6.8836	19.6	41.7	27.7
			19.6	-	30.0
VES 33	3.1923	6.8836	14.0	66.0	33.8
VES 34	3.1924	6.8836	13.6	-	52.2
Value Range (Profile C)			6.9-14.0	36.7-66.0	27.7-71.7
VES 35	3.1940	6.8843	41.4	-	65.8
VES 36	3.1943	6.8843	13.6	68.6	26.6
VES 37	3.1930	6.8834	3.6	61.0	50.2
			3.6	-	100.0
VES 38	3.1933	6.8825	4.6	27.2	70.9
			4.6	-	80.7
VES 39	3.1941	6.8831	8.9	29.5	35.2
			8.9	-	49.1
VES 40	3.1931	6.8834	6.3	22.7	20.8

Table 1 contd.

			6.3	-	64.8
VES 41	3.1930	6.8826	5.0	28.4	56.6
			5.0	-	36.6
VES 42	3.1933	6.8822	11.2	43.3	26.0
VES 43	3.1948	6.8854	7.0	39.3	31.4
VES 44	3.1936	6.8834	3.2	44.1	28.8
VES 45	3.1942	6.8841	4.5	63.7	18.5
VES 46	3.1927	6.8834	7.0	71.9	40.4
Value Range (Profile D)			3.2-41.4	22.7-71.9	18.5-100.0
VES 47	3.1928	6.8847	4.9	50.1	24.6
			4.9	-	62.9
VES 48	3.2094	6.8999	12.1	45.0	61.3
VES 49	3.2020	6.9005	3.8	33.1	26.7
			3.8	-	51.2
VES 50	3.1984	6.8921	4.9	4.6	38.5
			4.9	-	84.4
VES 51	3.1984	6.8921	15.3	55.8	31.9
VES 52	3.2012	6.9007	39.9	47.5	10.3
VES 53	3.1929	6.8844	59.4	81.0	15.9
VES 54	3.2021	6.8898	36.0	-	14.6
VES 55	3.1985	6.8857	31.2	35.1	12.0
VES 56	3.2034	6.8848	7.7	15.3	14.9
VES 57	3.1914	6.8934	6.3	26.9	41.7
			6.3	-	95.6
VES 58	3.1984	6.8866	5.8	26.4	14.8
			5.8	-	63.0
VES 59	3.1929	6.8994	5.6	20.2	23.3
			5.6	-	77.9
Value Range (Profile E)			3.8-59.4	15.3-81.0	10.3-95.6
VES 60	3.2034	6.8999	4.4	29.7	53.8
			4.4	-	95.0
VES 61	3.2020	6.9007	4.3	15.1	14.7
			4.3	-	67.6
VES 62	3.2032	6.8998	39.0	61.1	11.1
Value Range (Profile F)			4.3-39.0	15.1-61.1	11.1-95.0

Table 2. Results obtained from direct measurement.

Sample Type	Resistivity (kΩ-m) at 12V	Resistivity ((kΩ-m) at 24V	Permeability ($ms^{-1}x\ 10^{-6}$)	Bulk Density (gcm^{-3})
A	15.41	15.62	2.34	1.714
B	97.60	97.40	6.67	1.449
C	171.23	164.38	7.99	1.263
D	11.82	12.33	1.60	1.445
E	14.90	14.79	1.79	1.298
F	6.16	6.16	1.47	1.350
G	35.62	35.76	4.47	1.900
H	44.18	43.97	4.64	1.400

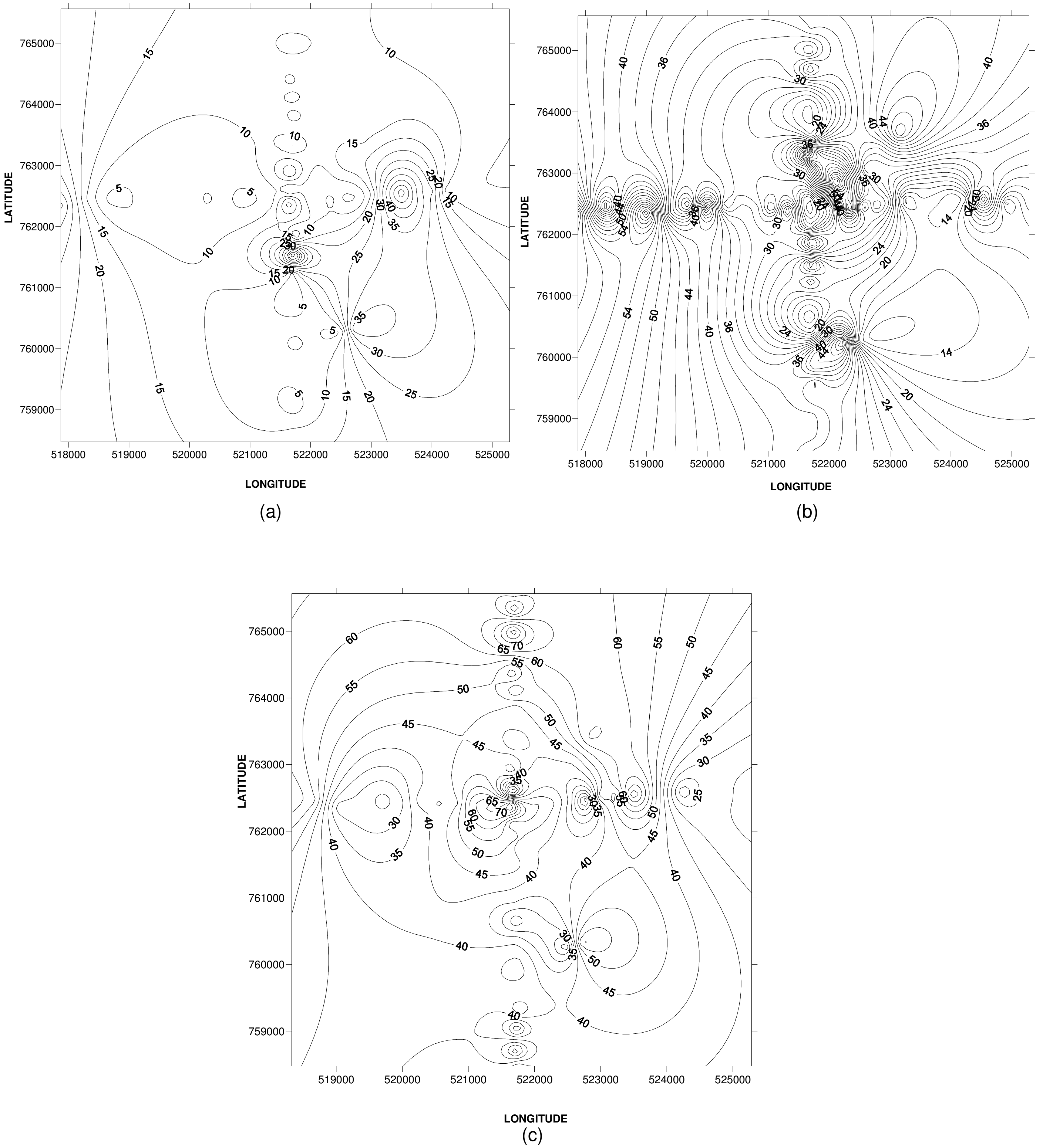

Figure 6. Contour maps showing: (a) overburden thickness; (b) limestone resistivity and; (c) limestone thickness.

The geoelectric profiles also showed the presence of continuous distribution of limestone of appreciable thickness coupled with the overburden thickness, with ample reserves of different qualities as observed from their va-

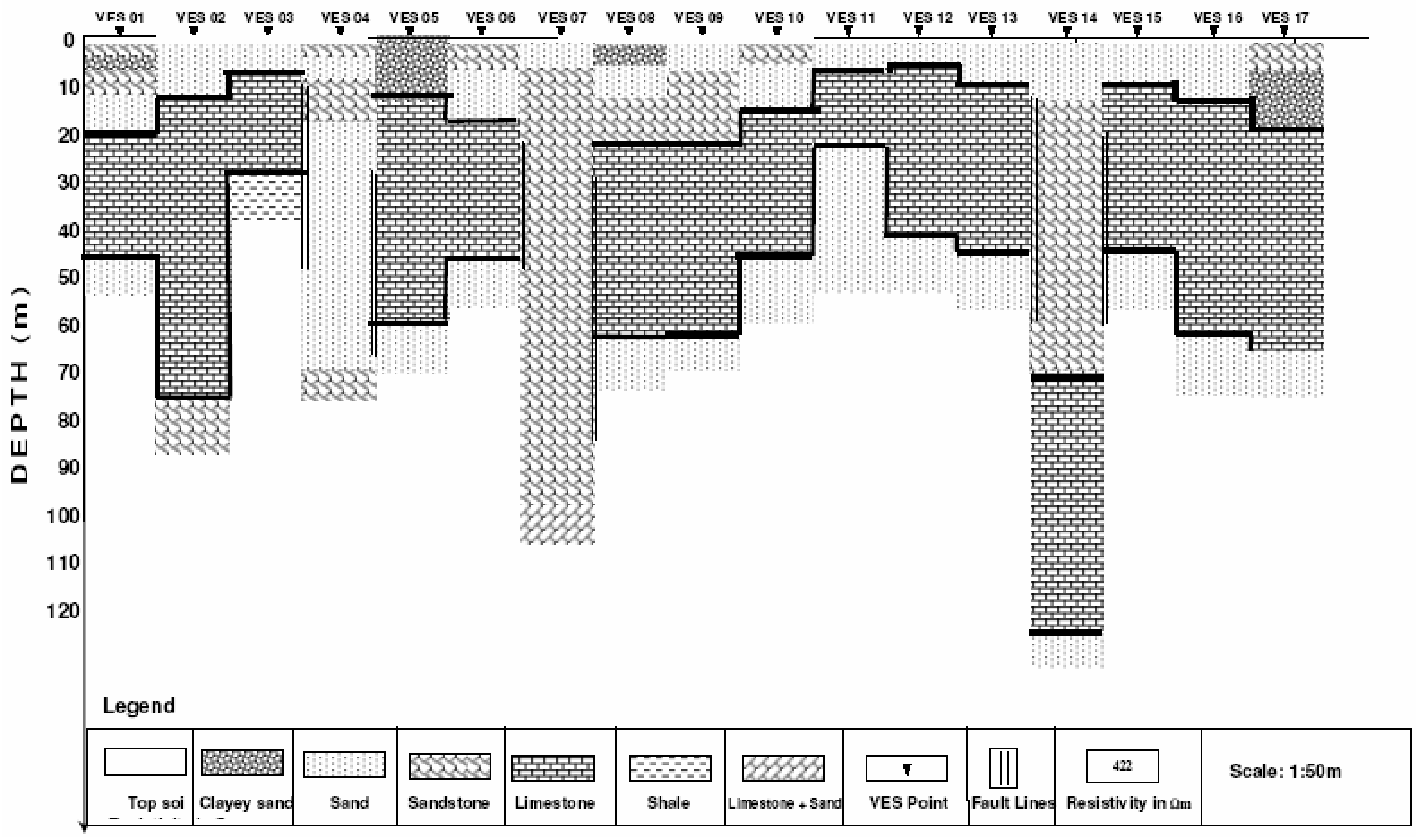

Figure 7a. Geo-electric Profile Beneath VES 01 – 17.

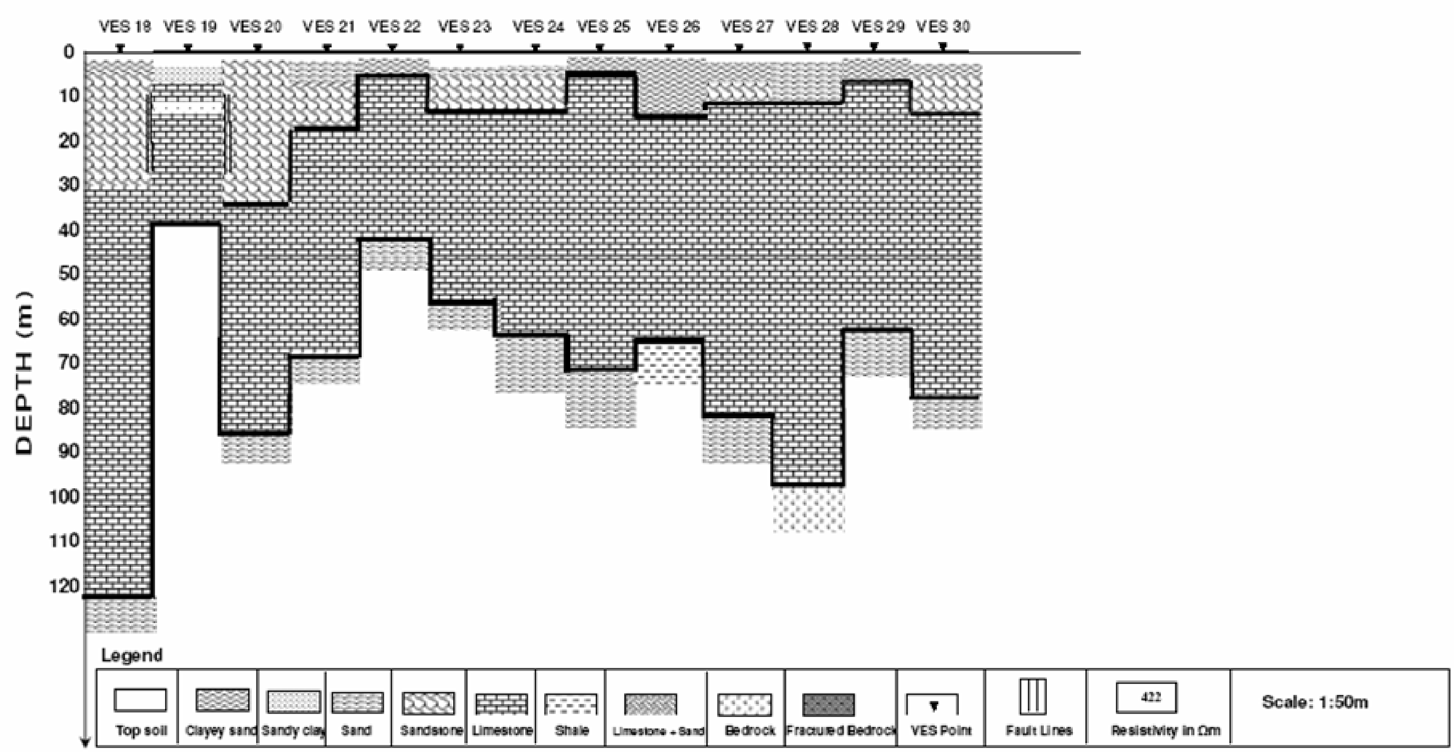

Figure 7b. Geoelectric Profile Beneath VES 18 – 30.

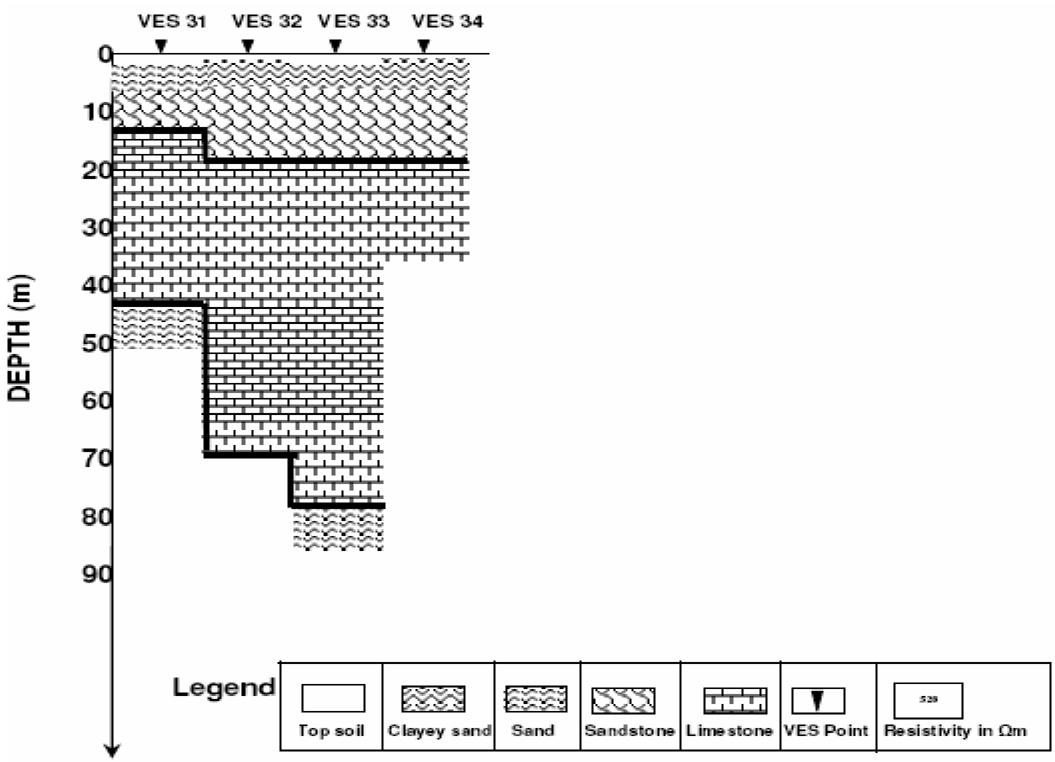

Figure 7c. Geoelectric profile beneath VES 31- 34.

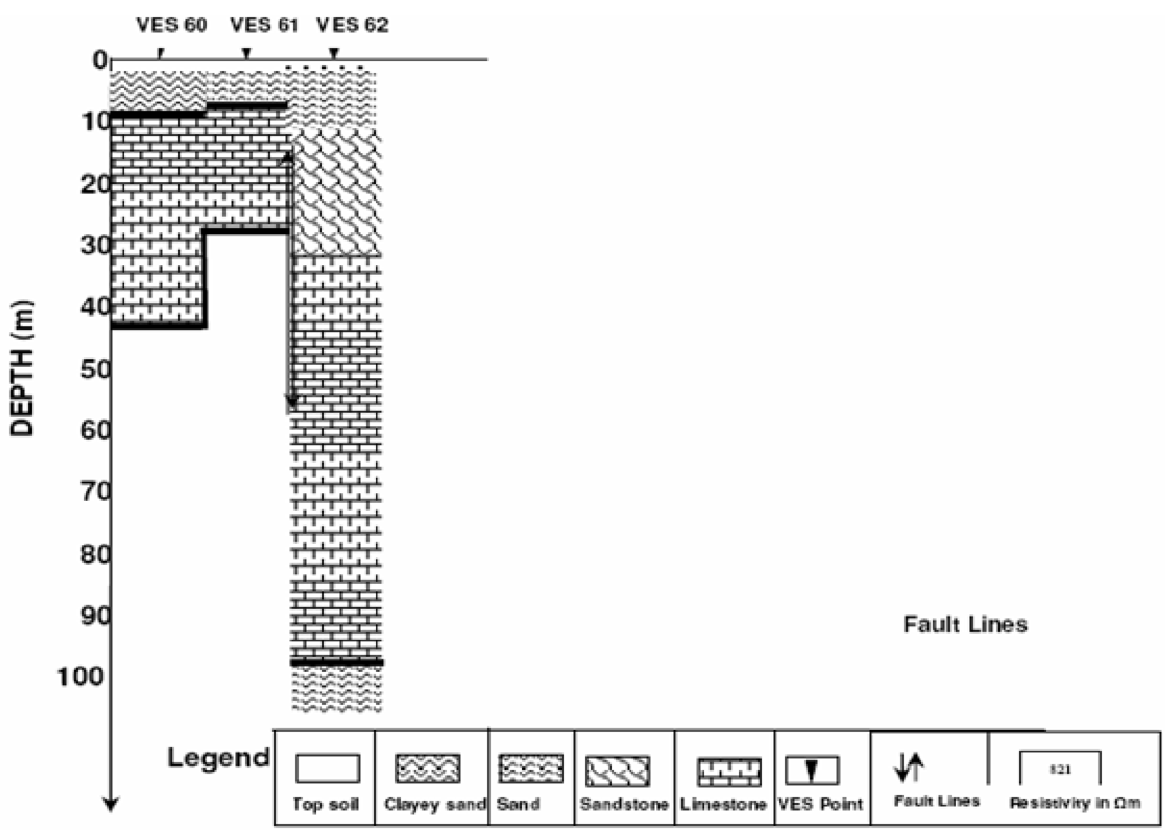

Figure 7d. Geoelectric Profile Beneath VES 60 – 62.

rious resistivity values.

Limestone characterization using laboratory direct method

Table 2 shows the resistivity values, permeability values and bulk density as obtained from the simple laboratory direct measurement using a direct current supply of 12 and 24 V. The resistivity values range between 6.2 - 171.2 kΩm at 12 V supply and 6.2 - 164.4 kΩm at 24 V. For the resistivity measurements, there is no significant difference between the values obtained for all the rock samples collected. However, all rock samples revealed a significant difference for both permeability and bulk density values. For hydraulic conductivity, the formula below was used:

$$K_{sat} = VL/ATY$$

where:

A = area = πr^2
R = radius of the core sampler
V = volume of water that passes the soil within 3 minutes
Y = L + H
L = length of soil inside the core sample
H = length of water from the top of the soil inside the core sampler
T = time of water run off
K_{sat} = saturated hydraulic conductivity

Badmus and Ayolabi (2005) already characterized the limestone into various litho-facies on the basis of resistivity variations; which is now correlated with the results obtained from the direct laboratory measurement. From this result, samples B and C are characterized as facie I because of their high values of permeability as well as resistivity. Sample G and H belong to facie II, which revealed limestone with high compaction and of low economic quality (Table 2).

Samples A, D and E belong to facie III because the resistivity and permeability values revealed that the limestone here is porous with grains as confirmed by Badmus and Ayolabi (2005). While sample F belongs to facie IV with the lowest value of resistivity and highest value for permeability. The limestone here is confirmed to be highly porous with cracks of different degrees.

Conclusion

The resistivity values of limestone rock samples collected from the study area as revealed by the simple laboratory setup using direct current of 12 and 24 V showed that the limestone of Ewekoro formation has various degrees of qualities as characterized by their resistivity and permeability values. This research work also showed to certain extents the accuracy of the electrical resistivity method of geophysical prospecting when compared with the results obtained in the work of Badmus and Ayolabi (2005). This research work further showed the occurrence of vast deposits of limestone, which can be of economic importance in mining and industrial purposes.

REFERENCES

Adegoke OS, Dessauvagie TFJ, Kogbe CA, Ogbe FGA (1971). Type section, Ewekoro Formation, biostratigraphy and microfacies., 4th African Micropal. Coll.Abidjan (1970) pp. 37-39.
Adegoke OS, Dessauvagie TFJ, Kogbe CA (1972). Radioactive age determination of glauconite from the type locality of the Ewekoro Formation. Conf. Afr. Geol. Ibadan (1970) 277-280.
Adegoke OS, Ogbe FGA, Jan Du Chene RE (1976). Excursion to the Ewekoro quarry (Paleocene-Eocene). Geol. Guide Nigerian Cretaceous-Recent Loc. pp. 1-17.
Badmus BS, Ayolabi EA (2005). Litho-facies changes in Ewekoro limestone using Schlumberger geoelectric sounding techniques. J. Appl. Sci. Technol. *(JAST)*, 10(1&2): 42–52.
Badmus BS, Ayanda JD, Popoola IO (2006). Geoelectric evaluation of Mica Schist deposits in Area J4 of Southwest, Nigeria. J. Appl. Sci. Technol. (JAST), 11(1&2): 39-43.
Jones HA, Hockey RD (1964). The geology of parts of Southwestern Nigeria. Geol. Survey Nig. Bull. 31: 22 – 24.
Kogbe CA (1976). The Cretaceous and Paleogene sediments of southern Nigeria. In C. A. Kogbe (Ed.) Geology of Nigeria. pp. 325-334.
Omatsola ME, Adegoke OS (1981). Tectonic Evaluation and cretaceous stratigraphy of the Dahomey Basin, J. Min. Geol. 5(2): 78-83.
Oladeji BO (1992). Environmental analysis of Ewekoro Formation at the Shagamu Quarry. Nig. J. Min. Geol., 28(1): 148–156.
Ojelabi EA, Badmus BS, Salau AA (2002). Comparative Analysis of Wenner and Schlumberger Methods of Geoelectric Sounding in subsurface delineation and groundwater exploration-a case study, J. Geol. Soc. India, 60: 623-628.